ARTICLE Communicated by Roger Brockett

Estimating a State-Space Model from Point Process Observations

Anne C. Smith
asmith@neurostat.mgh.harvard.edu
Neuroscience Statistics Research Laboratory, Department of Anesthesia and Critical Care, Massachusetts General Hospital, Boston, MA 02114, U.S.A.

Emery N. Brown
brown@neurostat.mgh.harvard.edu
Neuroscience Statistics Research Laboratory, Department of Anesthesia and Critical Care, Massachusetts General Hospital, Boston, MA 02114, U.S.A., and Division of Health Sciences and Technology, Harvard Medical School/Massachusetts Institute of Technology, Cambridge, MA 02139, U.S.A.

A widely used signal processing paradigm is the state-space model. The state-space model is defined by two equations: an observation equation that describes how the hidden state or latent process is observed and a state equation that defines the evolution of the process through time. Inspired by neurophysiology experiments in which neural spiking activity is induced by an implicit (latent) stimulus, we develop an algorithm to estimate a state-space model observed through point process measurements. We represent the latent process modulating the neural spiking activity as a gaussian autoregressive model driven by an external stimulus. Given the latent process, neural spiking activity is characterized as a general point process defined by its conditional intensity function. We develop an approximate expectation-maximization (EM) algorithm to estimate the unobservable state-space process, its parameters, and the parameters of the point process. The EM algorithm combines a point process recursive nonlinear filter algorithm, the fixed interval smoothing algorithm, and the state-space covariance algorithm to compute the complete data log likelihood efficiently. We use a Kolmogorov-Smirnov test based on the time-rescaling theorem to evaluate agreement between the model and point process data. We illustrate the model with two simulated data examples: an ensemble of Poisson neurons driven by a common stimulus and a single neuron whose conditional intensity function is approximated as a local Bernoulli process.

 © 2003 Massachusetts Institute of Technology

1 Introduction

A widely used signal processing paradigm in many fields of science and engineering is the state-space model. The state-space model is defined by two equations: an observation equation that defines what is being measured or observed and a state equation that defines the evolution of the process through time. State-space models, also termed *latent process models* or *hidden Markov models*, have been used extensively in the analysis of continuous-valued data. For a linear gaussian observation process and a linear gaussian state equation with known parameters, the state-space estimation problem is solved using the well-known Kalman filter. Many extensions of this algorithm to both nongaussian, nonlinear state equations and nongaussian, nonlinear observation processes have been studied (Ljung & Söderström, 1987; Kay, 1988; Kitagawa & Gersh, 1996; Roweis & Ghahramani, 1999; Gharamani, 2001). An extension that has received less attention, and the one we study here, is the case in which the observation model is a point process.

This work is motivated by a data analysis problem that arises from a form of the stimulus-response experiments used in neurophysiology. In the stimulus-response experiment, a stimulus under the control of the experimenter is applied, and the response of the neural system, typically the neural spiking activity, is recorded. In many experiments, the stimulus is explicit, such as the position of a rat in its environment for hippocampal place cells (O'Keefe & Dostrovsky, 1971; Wilson & McNaughton, 1993), velocity of a moving object in the visual field of a fly H1 neuron (Bialek, Rieke, de Ruyter van Steveninck, & Warland, 1991), or light stimulation for retinal ganglion cells (Berry, Warland, & Meister, 1997). In other experiments, the stimulus is implicit, such as for a monkey executing a behavioral task in response to visual cues (Riehle, Grün, Diesmann, & Aertsen, 1997) or trace conditioning in the rabbit (McEchron, Weible, & Disterhoft, 2001). The neural spiking activity in implicit stimulus experiments is frequently analyzed by binning the spikes and plotting the peristimulus time histogram (PSTH). When several neurons are recorded in parallel, cross-correlations or unitary events analysis (Riehle et al., 1997; Grün, Diesmann, Grammont, Riehle, & Aertsen, 1999) have been used to analyze synchrony and changes in firing rates. Parametric model-based statistical analysis has been performed for the explicit stimuli of hippocampal place cells using position data (Brown, Frank, Tang, Quirk, & Wilson, 1998). However, specifying a model when the stimulus is latent or implicit is more challenging. State-space models suggest an approach to developing a model-based framework for analyzing stimulus-response experiments when the stimulus is implicit.

We develop an approach to estimating state-space models observed through a point process. We represent the latent (implicit) process modulating the neural spiking activity as a gaussian autoregressive model driven by an external stimulus. Given the latent process, neural spiking activity

is characterized as a general point process defined by its conditional intensity function. We will be concerned here with estimating the unobservable state or latent process, its parameters, and the parameters of the point process model. Several approaches have been taken to the problem of simultaneous state estimation and model parameter estimation, the latter being termed *system identification* (Roweis & Ghahramani, 1999). In this article, we present an approximate expectation-maximization (EM) algorithm (Dempster, Laird, & Rubin, 1977) to solve this simultaneous estimation problem. The approximate EM algorithm combines a point process recursive nonlinear filter algorithm, the fixed interval smoothing algorithm, and the state-space covariance algorithm to compute the complete data log likelihood efficiently. We use a Kolmogorov-Smirnov test based on the time-rescaling theorem to evaluate agreement between the model and point process data. We illustrate the algorithm with two simulated data examples: an ensemble of Poisson neurons driven by a common stimulus and a single neuron whose conditional intensity function is approximated as a local Bernoulli process.

2 Theory

2.1 Notation and the Point Process Conditional Intensity Function. Let $(0, T]$ be an observation interval during which we record the spiking activity of C neurons. Let $0 < u_{c1} < u_{c2} <, \ldots, < u_{cJ_c} \leq T$ be the set of J_c spike times (point process observations) from neuron c for $c = 1, \ldots, C$. For $t \in (0, T]$, let $N^c_{0,t}$ be the sample path of the spike times from neuron c in $(0, t]$. It is defined as the event $N^c_{0,t} = \{0 < u_{c1} < u_{c2}, \ldots, u_{cj} \leq t \bigcap N^c(t) = j\}$, where $N^c(t)$ is the number of spikes in $(0, t]$ and $j \leq J_c$. The sample path is a right continuous function that jumps 1 at the spike times and is constant otherwise (Snyder & Miller, 1991). This function tracks the location and number of spikes in $(0, t]$ and therefore contains all the information in the sequence of spike times. Let $N_{0,t} = \{N^1_{0,t}, \ldots, N^C_{0,t}\}$ be the ensemble spiking activity in $(0, t]$.

The spiking activity of each neuron can depend on the history of the ensemble, as well as that of the stimulus. To represent this dependence, we define the set of stimuli applied in $(0, t]$ as $S_{0,t} = \{0 < s_1 <, \ldots, < s_\ell \leq t\}$. Let $H_t = \{N_{0,t}, S_{0,t}\}$ be the history of all C neurons up to and including time t. To define a probability model for the neural spiking activity, we define the conditional intensity function for $t \in (0, T]$ as (Cox & Isham, 1980; Daley & Vere-Jones, 1988):

$$\lambda_c(t \mid H_t) = \lim_{\Delta \to 0} \frac{\Pr(N^c_{0,t+\Delta} - N^c_{0,t} = 1 \mid H_t)}{\Delta}. \tag{2.1}$$

The conditional intensity function is a history-dependent rate function that generalizes the definition of the Poisson rate (Cox & Isham, 1980; Daley &

Vere-Jones, 1988). If the point process is an inhomogeneous Poisson process, the conditional intensity function is $\lambda_c(t \mid H_t) = \lambda_c(t)$. It follows that $\lambda_c(t \mid H_t)\Delta$ is the probability of a spike in $[t, t + \Delta)$ when there is history dependence in the spike train. In survival analysis, the conditional intensity is termed the *hazard function* because, in this case, $\lambda_c(t \mid H_t)\Delta$ measures the probability of a failure or death in $[t, t + \Delta)$ given that the process has survived up to time t (Kalbfleisch & Prentice, 1980).

2.2 Latent Process Model, Sample Path Probability Density, and the Complete Data Likelihood. It is possible to define the latent process in continuous time. However, to simplify the notation for our filtering, smoothing, and EM algorithms, we assume that the latent process is defined on a discrete set of evenly spaced lattice points. To define the lattice, we choose K large, and divide $(0, T]$ into K intervals of equal width $\Delta = T/K$, so that there is at most one spike per interval. The latent process model is evaluated at $k\Delta$ for $k = 1, \ldots, K$. We also assume the stimulus inputs can be measured at a resolution of Δ.

We define the latent model as the first-order autoregressive model,

$$x_k = \rho x_{k-1} + \alpha I_k + \varepsilon_k, \tag{2.2}$$

where x_k is the unknown state at time $k\Delta$, ρ is a correlation coefficient, I_k is the indicator function that is 1 if there is a stimulus at $k\Delta$ and zero otherwise, α modulates the effect of the stimulus on the latent process, and ε_k is a gaussian random variable with mean zero and variance σ_ε^2. While more complex latent process models can certainly be defined, equation 2.2 is adequate to illustrate the essential features of our algorithm.

The joint probability density of the latent process is

$$\begin{aligned} p(x \mid \rho, \alpha, \sigma_\varepsilon^2) = &\left[\frac{(1-\rho^2)}{2\pi\sigma_\varepsilon^2}\right]^{\frac{1}{2}} \\ &\times \exp\left\{-\frac{1}{2}\left[\frac{(1-\rho^2)}{\sigma_\varepsilon^2}x_0^2 \right.\right. \\ &\left.\left. + \sum_{k=1}^{K}\frac{(x_k - \rho x_{k-1} - \alpha I_k)^2}{\sigma_\varepsilon^2}\right]\right\}, \end{aligned} \tag{2.3}$$

where $x = (x_0, x_1, \ldots, x_K)$.

We assume that the conditional intensity function is $\lambda_c(k\Delta \mid x_k, H_k^c, \theta_c^*)$, where θ_c^* is an unknown parameter. We can express the joint probability density of the sample path of neuron c conditional on the latent process as (Barbieri, Quirk, Frank, Wilson, & Brown, 2001; Brown, Barbieri, Ventura,

Kass, & Frank, 2002)

$$p(N^c_{0,T} \mid x, H^c_T, \theta^*_c) = \exp\left[\int_0^T \log \lambda_c(u \mid x(u), H^c_u, \theta^*_c)\, dN^c(u) - \int_0^T \lambda_c(u \mid x(u), H^c_u, \theta^*_c)\, du\right], \tag{2.4}$$

where $dN^c(u) = 1$ if there is a spike at u from neuron c and 0 otherwise. Under the assumption that the neurons in the ensemble are conditionally independent given the latent process, the joint probability density of the sample paths of the ensemble is

$$p(N_{0,T} \mid x, H_T, \theta^*) = \prod_{c=1}^{C} p(N^c_{0,T} \mid x, H^c_T, \theta^*_c), \tag{2.5}$$

where $\theta^* = (\theta^*_1, \ldots, \theta^*_C)$.

2.3 Parameter Estimation: Expectation-Maximization Algorithm. To illustrate the algorithm, we choose a simple form of the conditional intensity function. That is, we take the conditional intensity function for neuron c as

$$\lambda_c(k\Delta) = \exp(\mu_c + \beta_c x_k), \tag{2.6}$$

where μ_c is the log of the background firing rate and β_c is its gain parameter that governs how much the latent process modulates the firing rate of this neuron. Here we have $\theta^*_c = (\mu_c, \beta_c)$. Equations 2.3 and 2.6 define a doubly stochastic point process (Cox & Isham, 1980). If we condition on the latent process, then equation 2.6 defines an inhomogeneous Poisson process. Under this model, all the history dependence is through the stimulus. We let $\theta = (\rho, \alpha, \sigma^2_\varepsilon, \theta^*)$. Because our objective is to estimate the latent process, x, and to compute the maximum likelihood estimate of the model parameter, θ, we develop an EM algorithm (Dempster et al., 1977). In our EM algorithm, we treat the latent process x as the missing or unobserved quantity. The EM algorithm requires us to maximize the expectation of the complete data log likelihood. It follows from equations 2.3 and 2.6 that the complete data likelihood for our model is

$$p(N_{0,T}, x \mid \theta) = p(N_{0,T} \mid x, \theta^*) p(x \mid \rho, \alpha, \sigma^2_\varepsilon). \tag{2.7}$$

2.3.1 E-Step. At iteration $\ell+1$ of the algorithm, we compute in the E-step the expectation of the complete data log likelihood given H_K, the ensemble

spiking activity and stimulus activity in $(0, T]$, and $\theta^{(\ell)}$, the parameter estimate from iteration ℓ. By our notation convention in the previous section, since $K\Delta = T$, $H_K = H_T$ and

$$\begin{aligned}
Q(\theta \mid \theta^{\ell}) &= \mathrm{E}[\log[p(N_{0,T}, x \mid \theta)] \parallel H_K, \theta^{(\ell)}] \\
&= \mathrm{E}\left[\sum_{k=0}^{K}\sum_{c=1}^{C}(dN^c(k\Delta)(\mu_c + \beta_c x_k + \log\Delta)\right. \\
&\qquad \left. - \exp(\mu_c + \beta_c x_k)\Delta) \parallel H_K, \theta^{(\ell)}\right] \\
&\quad + \mathrm{E}\left[\sum_{k=1}^{K} -\frac{1}{2}\frac{(x_k - \rho x_{k-1} - \alpha I_k)^2}{\sigma_\varepsilon^2}\right. \\
&\qquad \left. -\frac{K}{2}\log 2\pi - \frac{K}{2}\log\sigma_\varepsilon^2 \parallel H_K, \theta^{(\ell)}\right] \\
&\quad + \mathrm{E}\left[\frac{1}{2}\log(1-\rho^2) - \frac{1}{2}\frac{x_0^2(1-\rho^2)}{\sigma_\varepsilon^2} \parallel H_K, \theta^{(\ell)}\right]. \qquad (2.8)
\end{aligned}$$

Upon expanding the right side of equation 2.8, we see that calculating the expected value of the complete data log likelihood requires computing the expected value of the latent process $\mathrm{E}[x_k \parallel H_K, \theta^{(\ell)}]$ and the covariances $\mathrm{E}[x_k^2 \parallel H_K, \theta^{(\ell)}]$ and $E[x_k x_{k+1} \parallel H_K, \theta^{(\ell)}]$. We denote them as

$$x_{k|K} \equiv \mathrm{E}[x_k \parallel H_K, \theta^{(\ell)}] \qquad (2.9)$$

$$W_k \equiv \mathrm{E}[x_k^2 \parallel H_K, \theta^{(\ell)}] \qquad (2.10)$$

$$W_{k,k+1} \equiv E[x_k x_{k+1} \parallel H_K, \theta^{(\ell)}], \qquad (2.11)$$

for $k = 1, \ldots, K$ where the notation $k \mid j$ denotes the expectation of the latent process at $k\Delta$ given the ensemble spiking activity and the stimulus up to time $j\Delta$. To compute these quantities efficiently, we decompose the E-step into three parts: a forward nonlinear recursive filter to compute $x_{k|k}$; a backward, fixed interval smoothing (FIS) algorithm to estimate $x_{k|K}$; and a state-space covariance algorithm to estimate W_k and $W_{k,k+1}$. This approach for evaluating the complete data log likelihood was suggested first by Shumway and Stoffer (1982). They used the FIS but a more complicated form of the state-covariance algorithm. An alternative covariance algorithm was given in Brown (1987). The logic of this approach is to compute the forward mean and covariance estimates and combine them with the backward mean and covariance estimates to obtain equations 2.10 and 2.11. This approach is exact for linear gaussian latent process models and linear gaussian

observation processes. For our model, it will be approximate because our observations form a point process.

E-Step I: Nonlinear Recursive Filter. The following equations comprise a recursive nonlinear filtering algorithm to estimate $x_{k|k}$ and $\sigma^2_{k|k}$ using equation 2.6 as the conditional intensity. The algorithm is based on the maximum a posterori derivation of the Kalman filter algorithm (Mendel, 1995; Brown et al., 1998). It recursively computes a gaussian approximation to the posterior probability density $p(x_k \mid H_k, \theta^{(\ell)})$. The approximation is based on recursively computing the posterior mode $x_{k|k}$ and computing its variance $\sigma^2_{k|k}$ as the negative inverse of the second derivative of the log posterior probability density (Tanner, 1996). The nonlinear recursive algorithm is:

(Observation Equation)

$$p(dN(k\Delta) \mid x_k) = \prod_{c=1}^{C} [\exp(\mu_c + \beta_c x_k)\Delta]^{dN^c(k\Delta)} \times \exp(-\exp(\mu_c + \beta_c x_k)\Delta) \tag{2.12}$$

(One-Step Prediction)

$$x_{k|k-1} = \rho x_{k-1|k-1} + \alpha I_k \tag{2.13}$$

(One-Step Prediction Variance)

$$\sigma^2_{k|k-1} = \rho^2 \sigma^2_{k-1|k-1} + \sigma^2_\varepsilon \tag{2.14}$$

(Posterior Mode)

$$x_{k|k} = x_{k|k-1} + \sigma^2_{k|k-1} \sum_{c=1}^{C} \beta_c [dN^c(k\Delta) - \exp(\mu_c + \beta_c x_{k|k})\Delta] \tag{2.15}$$

(Posterior Variance)

$$\sigma^2_{k|k} = -\left[-(\sigma^2_{k|k-1})^{-1} - \sum_{i=1}^{C} \beta_c^2 \exp(\mu_c + \beta_c x_{k|k})\Delta \right]^{-1} \tag{2.16}$$

for $k = 1, \ldots, K$. The initial condition is x_0 and $\sigma^2_{0|0} = \sigma^2_\varepsilon (1 - \rho^2)^{-1}$. The algorithm is nonlinear because $x_{k|k}$ appears on the left and right of equation 2.15. The derivation of this algorithm for an arbitrary point process model is given in the appendix.

E-Step II: Fixed Interval Smoothing (FIS) Algorithm. Given the sequence of posterior mode estimates $x_{k|k}$ (see equation 2.15) and the variance $\sigma^2_{k|k}$ (see

equation 2.16) we use the fixed interval smoothing algorithm to compute $x_{k|K}$ and $\sigma^2_{k|K}$. The algorithm is (Mendel, 1995; Brown et al., 1998)

$$x_{k|K} = x_{k|k} + A_k(x_{k+1|K} - x_{k+1|k}), \tag{2.17}$$

where

$$A_k = \rho\sigma^2_{k|k}(\sigma^2_{k+1|k})^{-1} \tag{2.18}$$

and

$$\sigma^2_{k|K} = \sigma^2_{k|k} + A^2_k(\sigma^2_{k+1|K} - \sigma^2_{k+1|k}) \tag{2.19}$$

for $k = K-1, \ldots, 1$ and initial conditions $x_{K|K}$ and $\sigma^2_{K|K}$.

E-Step III: State-Space Covariance Algorithm. The covariance estimate, $\sigma_{k,u|K}$, can be computed from the state-space covariance algorithm (de Jong & MacKinnon, 1988) and is given as

$$\sigma_{k,u|K} = A_k\sigma_{k+1,u|K} \tag{2.20}$$

for $1 \le k \le u \le K$. It follows that the covariance terms required for the E-step are

$$W_{k,k+1} = \sigma_{k,k+1|K} + x_{k|K}x_{k+1|K} \tag{2.21}$$

and

$$W_k = \sigma^2_{k|K} + x^2_{k|K}. \tag{2.22}$$

2.3.2 M-Step. In the M-step, we maximize the expected value of the complete data log likelihood in equation 2.8 with respect to $\theta^{(\ell+1)}$. In so doing, we obtain the following closed-form solutions for $\rho^{(\ell+1)}$, $\alpha^{(\ell+1)}$ and $\sigma_\varepsilon^{2(\ell+1)}$,

$$\begin{bmatrix} \rho^{(\ell+1)} \\ \alpha^{(\ell+1)} \end{bmatrix} = \begin{bmatrix} \sum_{k=1}^{K} W_{k-1} & \sum_{k=1}^{K} x_{k-1|k}I_k \\ \sum_{k=1}^{K} x_{k-1|k}I_k & \sum_{k=1}^{K} I_k \end{bmatrix}^{-1} \begin{bmatrix} \sum_{k=1}^{K} W_{k,k-1} \\ \sum_{k=1}^{K} x_{k|k}I_k \end{bmatrix} \tag{2.23}$$

$$\sigma_\varepsilon^{2(\ell+1)} = K^{-1}\left[\sum_{k=1}^{K} W_k + \rho^{2(\ell+1)}\sum_{k=1}^{K} W_{k-1} + \alpha^{2(\ell+1)}\sum_{k=1}^{K} I_k\right.$$

$$- 2\rho^{(\ell+1)} \sum_{k=1}^{K} W_{k,k-1} - 2\alpha^{(\ell+1)} \sum_{k=1}^{K} x_{k|K} I_k + 2\rho^{(\ell+1)} \alpha^{(\ell+1)}$$

$$\times \sum_{k=1}^{K} x_{k-1|K} I_k + W_0 \left(1 - \rho^{2(\ell+1)}\right) \Bigg], \tag{2.24}$$

where initial conditions for the latent process are estimated from $x_0^{(\ell+1)} = \rho^{(\ell+1)} x_{1|K}$ and $\sigma_{0|0}^{2(\ell+1)} = \sigma_\varepsilon^{2(\ell+1)} (1 - \rho^{2(\ell+1)})^{-1}$. The closed-form solution for $\rho^{(\ell+1)}$ in equation 2.23 is obtained by neglecting the last two terms in the expectation of the complete data log likelihood (see equation 2.8). This approximation means that we estimate $\rho^{(\ell+1)}$ from the probability density of $x_1, \ldots, x_K$ given x_0 and the point process measurements instead of the probability density of $x_0, \ldots, x_K$ given the point process measurements. Inclusion of the last two terms results in a cubic equation for computing $\rho^{(\ell+1)}$, which is avoided by using the closed-form approximation. We report only the results of the closed-form solution in section 3 because we found that for our algorithms, the absolute value of the fractional difference between the two solutions was less than 10^{-6} (i.e., |cubic solution-closed form solution|/cubic solution $< 10^{-6}$).

The parameter $\mu_c^{(\ell+1)}$ is estimated as

$$\mu_c^{(\ell+1)} = \log N^c(T) - \log \left(\sum_{k=1}^{K} \exp \left(\beta_c^{(\ell+1)} x_{k|K} + \frac{1}{2} \beta_c^{2(\ell+1)} \sigma_{k|K}^2 \right) \Delta \right), \tag{2.25}$$

whereas $\beta_c^{(\ell+1)}$ is the solution to the nonlinear equation,

$$\sum_{k=1}^{K} dN^c(k\Delta) x_{k|K} = \exp \mu_c^{(\ell+1)} \left\{ \sum_{k=1}^{K} \exp \left(\beta_c^{(\ell+1)} x_{k|K} + \frac{1}{2} \beta_c^{(\ell+1)} \sigma_{k|K}^2 \right) \times (x_{k|K} + \beta_c^{(\ell+1)} \sigma_{k|K}^2) \Delta \right\}, \tag{2.26}$$

which is solved by Newton's method after substituting $\mu_c^{(\ell+1)}$ from equation 2.26. The expectations needed to derive equations 2.25 and 2.26 were computed using the lognormal probability density and the approximation of $p(x_k \mid H_K, \theta^{(\ell)})$ as a gaussian probability density with mean $x_{k|K}$ and variance $\sigma_{k|K}^2$.

2.4 Assessing Model Goodness-of-Fit by the Time-Rescaling Theorem. The latent process and point process models, along with the EM algorithm, provide a model and an estimation procedure for computing the latent process and the parameter vector θ. It is important to evaluate model goodness-of-fit, that is, determine how well the model describes the neural spike train data series data. Because the spike train models are defined in terms of an explicit point process model, we can use the time-rescaling theorem to evaluate model goodness-of-fit. To do this, we compute for each neuron the time-rescaled or transformed interspike intervals

$$\tau_j = \int_{u_{j-1}}^{u_j} \lambda(u \mid \hat{\theta})\, du, \tag{2.27}$$

where the u_js are the spike times from the neuron and $\lambda(t \mid \theta)$ is the conditional intensity function in equation 2.6 evaluated at the maximum likelihood estimate $\hat{\theta}$ for $j = 1, \ldots, J$, where we have dropped the subscript c to simplify notation. The u_js are a point process with a well-defined conditional intensity function and, hence, by the time-rescaling theorem, the τ_js are independent, exponential random variables with a unit rate (Barbieri et al., 2001; Brown et al., 2002). Under the further transformation $z_j = 1 - \exp(-\tau_j)$, the z_js are independent, uniform random variables on the interval (0,1). Therefore, we can construct a Kolmogorov-Smirnov (K-S) test to measure agreement between the z_js and the uniform probability density (Barbieri et al., 2001; Brown et al., 2002). First, we order the z_js from the smallest to the largest value. Then we plot values of the cumulative distribution function of the uniform density defined as $b_j = \frac{j-\frac{1}{2}}{J}$ for $j = 1, \ldots, J$ against the ordered z_js. The points should lie on the 45 degree line. Because the transformation from the u_js to the z_js is one-to-one, a close agreement between the probability density of the z_js and the uniform probability density on (0,1) indicates close agreement between the (latent process-point process) model and the point process measurements. Hence, the time-rescaling theorem provides a direct means of measuring agreement between a point process or neural spike train time series and a probability model intended to describe its stochastic structure.

3 Applications

3.1 Example 1. Multiple Neurons Driven by a Common Latent Process. To illustrate our analysis paradigm, we simulate $C = 20$ simultaneously recorded neurons from the model described by equations 2.2 and 2.6. The time interval for the simulation was $T = 10$ seconds, and the latent process model parameters were $\rho = 0.99$, $\alpha = 3$, and $\sigma_\varepsilon^2 = 10^{-3}$ with the implicit stimulus I_k applied at 1 second intervals. The parameters for the conditional intensity function defining the observation process were the log of the background firing rate $\mu = -4.9$ for all neurons, whereas the gain coefficients

Table 1: True Parameter Values and EM Algorithm Parameter Estimates.

Parameter	True	Estimate	Parameter	True	Estimate
ρ	0.990	0.993	β_{10}	1.079	1.190
α	3.000	2.625	β_{11}	1.008	1.039
μ	−4.900	−5.105	β_{12}	1.078	1.247
β_1	1.075	1.261	β_{13}	1.009	1.031
β_2	0.989	1.060	β_{14}	1.078	1.129
β_3	1.035	1.039	β_{15}	0.980	1.121
β_4	0.973	1.101	β_{16}	0.976	1.164
β_5	1.003	1.190	β_{17}	0.990	1.234
β_6	0.992	1.132	β_{18}	0.968	1.154
β_7	0.977	1.118	β_{19}	0.956	0.979
β_8	1.027	1.176	β_{20}	1.098	1.350
β_9	1.066	1.089			

β_c for the 20 neurons were chosen randomly on the interval [0.9 1.1]. These parameter values for the latent and observation processes were chosen to give an approximate average firing rate of 10 Hz for each neuron. The neural spike trains were simulated using the time-rescaling theorem algorithm described in Brown et al. (2002), and the state equations in the EM algorithm were updated at $\Delta = 1$ msec.

Using the EM algorithm described in the previous section, we fit the model in equations 2.2 and 2.6 simultaneously to the 20 simulated neural spike trains, assuming a fixed noise variance, $\sigma_\varepsilon^2 = 10^{-3}$. The convergence criteria for the algorithm were absolute changes of less than 10^{-2} in consecutive iterates of the parameters and relative changes in the parameter iterates of less than 10^{-3}, that is, $|old - new|/old < 10^{-3}$. The parameter estimates from the EM algorithm were in good agreement with the true values used to simulate the spike train data (see Table 1). In this case, the overestimates of the gain coefficients, β_c, are offset by the underestimates of α and μ.

Approximating the probability density of the state at $k\Delta$ as the gaussian density with mean $\hat{x}_k$ and variance, $\hat{\sigma}_k^2$, it follows from equation 2.6 and the standard change of variables formula from probability theory that the probability density of the rate for neuron c at time $k\Delta$ is the lognormal probability density defined as

$$p(\lambda_k^c \mid \hat{\mu}_c, \hat{\beta}_c, \hat{x}_k) = (2\pi\hat{\sigma}_k^2)^{-\frac{1}{2}}\hat{\beta}_c(\lambda_k^c)^{-1} \times \exp\left(-\frac{1}{2}\left[\frac{\hat{\beta}_c^{-1}(\log\lambda_k^c - \hat{\mu}_c) - \hat{x}_k}{\hat{\sigma}_k}\right]^2\right), \tag{3.1}$$

where $\hat{\mu}_c$ and $\hat{\beta}_c$ are the EM algorithm estimates of μ_c and β_c for $c = 1, \ldots, 20$. The $1 - \xi$ confidence limits for the rate are computed simply by using the

relation between the lognormal and standard gaussian probabilities to find the $\xi/2$ and $1-\xi/2$ quantiles of the probability density in equation 3.1 for $\xi \in (0,1)$. In our analyses, we take $\xi = 0.05$ and construct 95% confidence intervals.

To compare our model-based analysis with current practices for analyzing neural spike train data using empirical smoothing methods, we also estimated the rate function for each of the 20 neurons by dividing the number of spikes in a 100 msec window by 100 msec. The window was then shifted 1 msec to give the same temporal resolution as in our updating algorithms. Because the latent process drives all the neurons, we also estimated the population rate by averaging the rates across all 20 neurons. This is a commonly used empirical temporal smoothing algorithm for computing spike rate that does not make use of stimulus information in the estimation (Riehle et al., 1997; Grün et al., 1999; Wood, Dudchenko, & Eichenbaum, 1999).

The confidence limits of the model-based rate function give a good estimate of the true firing rate used to generate the spikes (see Figure 1). In particular, the estimates reproduce the magnitude and duration of the effect of the implicit stimulus on the spike firing rate. The population firing rate estimated using temporal smoothing across all neurons is misleading (see Figure 1, dot-dashed line) in that around the time of the stimuli, it has diminished amplitude and is spread out in time. Furthermore, if we smooth a single spike train without averaging across neurons, spurious peaks in the firing rate can be produced due to noise (see Figure 1, solid gray line). By using information about the timing of the stimulus, the model firing rate estimate follows the true rate function more closely.

The 95% confidence bounds for the state process estimated from the EM algorithm cover almost completely the time course of the true state process (see Figure 2). The true state lies sometimes outside the confidence limits in regions where there are very few spikes and, hence, little information about the latent process.

To assess how well the model fits the data, we apply the K-S goodness-of-fit tests based on the time-rescaling theorem as described in section 2.4 (see Figure 3). In Figures 3A, 3B, and 3C, the solid black line represents exact agreement between the model and spike data, and dotted lines represent 95% confidence limits. For 18 of 20 neurons, the model lies within the confidence limits, indicating a good fit to the data. In contrast, for 14 of the 20 neurons, the empirical estimate lies outside the confidence limits. For 6 of 20 neurons, both the model and empirical estimates lie within the confidence limits (see Figure 3B). In two cases, the model lies outside the confidence limits (see Figure 3C). In both cases where the model does not fit the data, the empirical estimate does not either. Thus, the model appears to give a considerably more accurate description of the spike train than the empirical estimate.

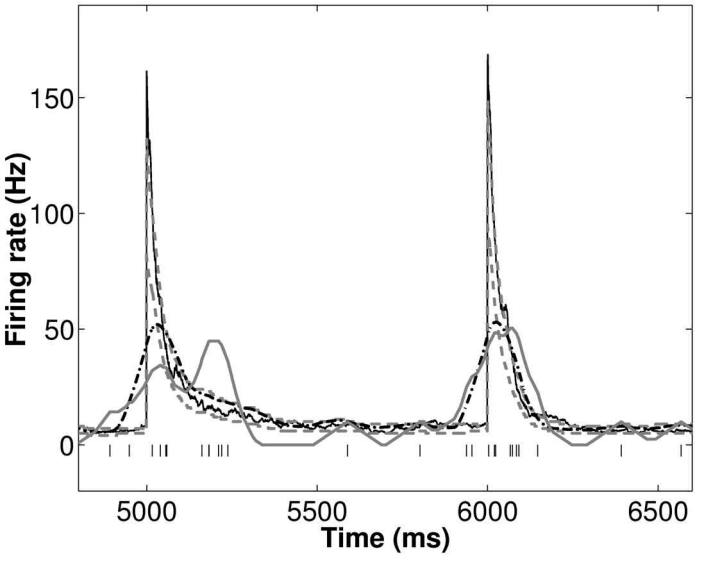

Figure 1: A 2000 millisecond segment of data from neuron 8 in the 20-neuron simulation study of latent process estimation by the EM algorithm from example 1. During this period, 26 spikes (vertical bars above abscissa) are concentrated around two stimulus events at 5000 msec and 6000 msec. The 95% confidence bands for the firing rate estimated by the latent model (dashed lines) cover the true rate (solid black line) used to generate the spikes most of the time. In contrast, when the firing rate for neuron 8 is estimated empirically (solid gray line) using a 100 msec smoothing window (i.e., by dividing the number of spikes in a 100 msec window by 100 msec), the stimuli appear diminished in amplitude and spread out in time. Furthermore, a spurious third peak in firing rate is produced approximately 200 ms after the true first peak. This third peak is avoided by using a smoothed estimate that is averaged over all cells (dash-dotted black line), but the EM algorithm estimate of the firing rate based on the model more accurately reproduces the features of the stimuli.

3.2 Example 2. Single Neuron Latent Stimulus-Response Model. A common practice is to use the binomial probability mass function as a local model for analyzing neural spike trains. We demonstrate how the parameters of a local Bernoulli model may be estimated using our EM algorithm. We generate a single spike train subject to multiple repeated stimuli over a period of approximately 1 minute. In this example, the conditional intensity is given by

$$\lambda(k\Delta)\Delta = \exp(\mu + x_k)\Delta \approx \frac{\exp(\mu + x_k)\Delta}{1 + \exp(\mu + x_k)\Delta} = p_k, \tag{3.2}$$

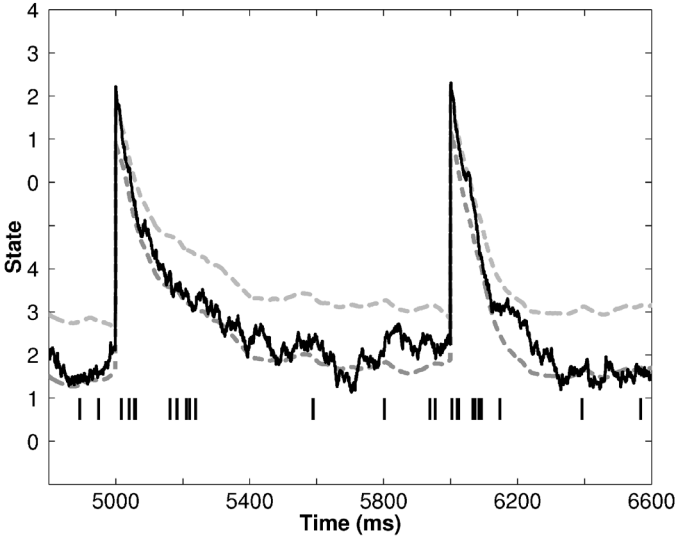

Figure 2: True state (solid black line) and estimated 95% confidence limits (dashed lines) for the true state computed from the spike train observed in Figure 1 using the EM algorithm. The estimated confidence limits computed as $x_{k|k} \pm 1.96\sigma_{k|k}$ fail to cover the true state when few spikes are discharged (e.g., near 5700 ms).

Figure 3: *Facing page.* Kolmogorov-Smirnov goodness-of-fit analyses based on the time-rescaling theorem for three representative neurons. Each panel is the K-S plots comparing the model rate estimate (dashed line), the empirical rate estimate (solid gray line), and the true rate (solid black line). In these figures, the 45 degree line in black represents an exact agreement between the model and the spike data. Dotted lines in each panel are the 95% confidence limits (see Brown et al., 2002, for details). Since the true rate was used to generate spikes, the true rate KS plot always lies within the confidence limits. (A) An example of the KS plot from 1 of the 18 out of the 20 neurons for which the model-based estimate of the KS plot was entirely within the confidence limits, indicating close agreement between the overall model fit and the simulated data. (B) An example of 1 of the 6 out of the 20 neurons for which the K-S plot based on the empirical rate estimate completely lies within the 95% confidence limits. (C) An example of 1 of the 2 out of the 20 neurons for which the K-S plot based on the model estimate of the rate function fails to fall within the 95% confidence limits. For both of these neurons, as this panel suggests, the KS plot based on the empirical rate model did not remain in the 95% confidence bounds.

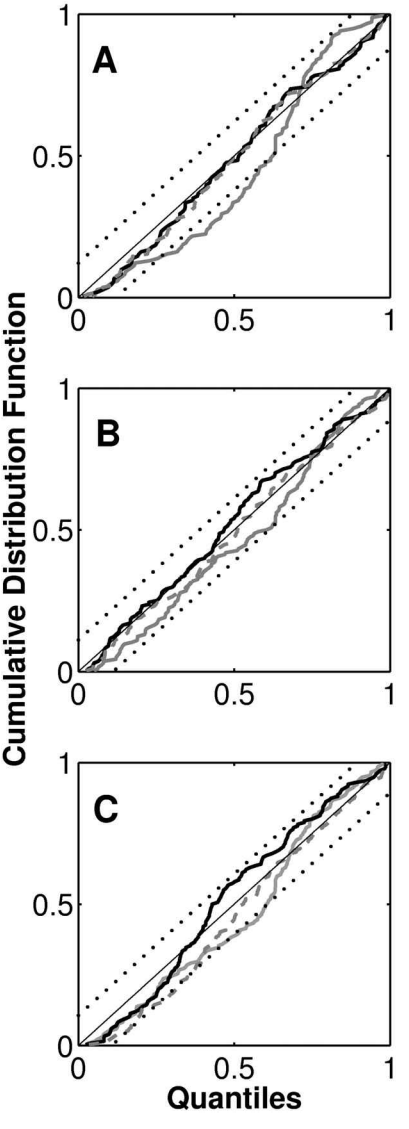

and spikes are generated with the local Bernoulli model,

$$p(dN(k\Delta) \mid H_k) = p_k^{dN(k\Delta)}(1-p_k)^{1-dN(k\Delta)}, \tag{3.3}$$

with parameters $\mu = -4.6$, $\alpha = 4$, and $\rho = 0.8$. The implicit stimulus is applied at 40 time points. We assume the noise σ_ε^2 in the latent process is 0.2. In this example, we set $\Delta = 5$ msec. This generates a spike train with

Table 2: True Parameter Values and the EM Algorithm Parameter Estimates.

Parameter	ρ	α	σ_ε^2	μ
True	0.800	4.000	0.200	−4.600
Estimate	0.804	3.573	0.125	−4.404

an average firing rate over the minute period of approximately 10 Hz. The parameters, including the noise variance σ_ε^2, are again estimated using the EM algorithm and are in good agreement with their true values (see Table 2).

As in the previous example, confidence intervals were computed for the true rate function by deriving the probability density function for λ_k using the standard change of variable formula. Firing rates estimated by the model are compared with the empirical temporally smoothed rate computed by counting spikes in a 100 msec window and then dividing by 100 msec.

The firing rate (95% confidence limits) computed by the model compares favorably with the original rate used to generate the spikes (see Figure 4). The 95% confidence limits for the model estimate the magnitude and shape of the stimulus effect on the rate even when the stimulus has little obvious effect on the spike train. This is because the estimates for each stimulus's effect are made based on the whole time series. In contrast, the temporally smoothed estimate of rate does not clearly identify stimulus effects on the spike train (see Figure 4, solid gray line). The choice of a 100 msec window for these simulated data appears too large as increases in firing rate at the stimuli are smoothed out. We can also make an overall estimate of the accuracy of the firing rates by comparing the model and the empirical firing rates with the true firing at the stimulus times, namely, at 40 points in time where we applied the stimulus during the 1 minute epoch of simulated data. The mean differences (standard error) between the empirical and model rates compared to the true rate at these times are −113.9 (4.5) Hz and −8.5 (4.4) Hz, respectively. Thus, the model provides a significantly better approximation to the true rate than the empirical method (Student's t-test, $p < 10^{-6}$). The estimate of the state variable is found to compare well with the true state used to generate the spike train (see Figure 5).

Again we assess model goodness-of-fit using the K-S plot (see Figure 6). The fit of model lies within the 95% confidence limits except at very small quantiles and follows closely the curve for the true firing rate. In contrast, the fit for the empirical 100 msec temporal smoothing method lies outside the confidence limits for a large portion of the total time, indicating poor fit to the distribution over low and high percentiles.

3.3 An Extension to More General Point Process and State-Space Models. In the two simulated data examples we considered, the log conditional intensity function $\log \lambda_c(t \mid H_t)$ was a linear function of both the state vari-

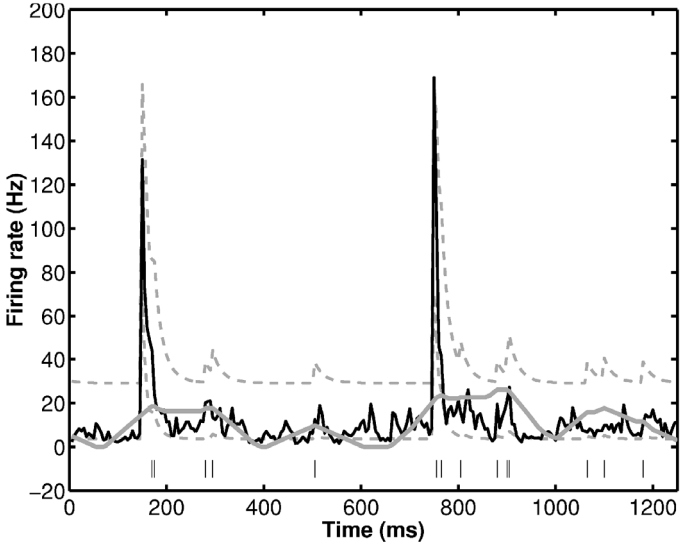

Figure 4: Simulated spike train (vertical bars above the abcissa), true firing rate (solid black line) from the local Bernoulli model (see equation 3.2) in example 2, 95% confidence limits for the rate from the model-based EM algorithm (dashed lines), and empirical firing rate estimate (solid gray line) computed by temporal smoothing over the 100 msec window. In this time segment, two external stimuli are applied at 150 msec and 750 msec. The 95% confidence limits cover nearly everywhere the true rate function. Although the spike count does not obviously increase at these times, the algorithm estimates effectively the amplitude and duration of the stimulus because it uses information from the entire spike train. The 100 msec window for the empirical rate function appears too large as increases in firing rate at the stimuli are smoothed out.

able x_k and certain components of the parameter vector θ. The EM algorithm is straightforward to modify when this is not the case. For an arbitrary $\lambda_c(t \mid H_t)$, the E-step in equation 2.8 becomes

$$\begin{aligned} Q(\theta \mid \theta^{(\ell)}) &= E[\log[p(N_{0,T}, x \mid \theta)] \parallel H_k, \theta^{(\ell)}] \\ &\approx E\left[\sum_{k=0}^{K}\sum_{c=1}^{C} dN^c(k\Delta)\log\lambda_c(x_k \mid H_k, \theta)\right. \\ &\qquad \left. - \lambda_c(x_k \mid H_k, \theta)\Delta \parallel H_K, \theta^{(\ell)}\right] \\ &\quad + E[\log p(x \mid \theta) \parallel H_K, \theta^{(\ell)}], \end{aligned} \tag{3.4}$$

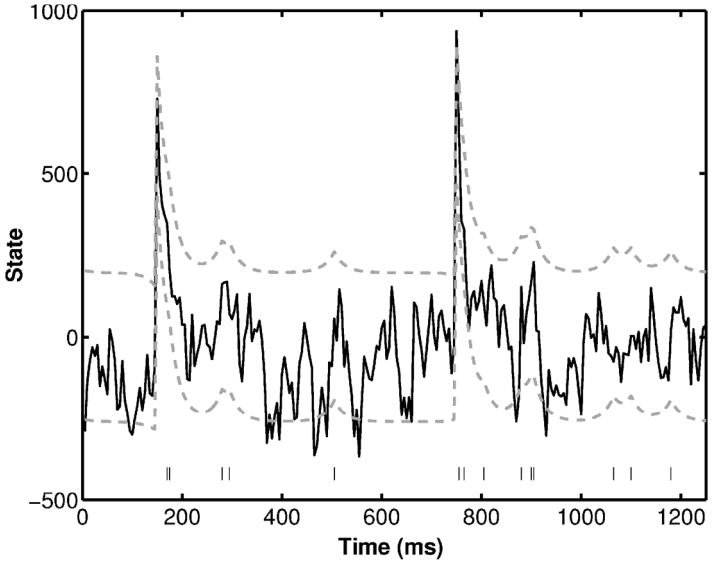

Figure 5: The true state (black line) and the model-based estimates of the 95% confidence intervals (dashed lines) computed using the EM algorithm for the local Bernoulli probability model corresponding to the spike train and rate function in Figure 4. As in example 1, Figure 5 shows that the 95% confidence limits cover the true state completely except when the neural spiking activity is low (around 700 msec).

where the last term in equation 3.4 is the sum of the last two terms on the right-hand side of equation 2.8. We assume $\lambda_c(x_k \mid H_k, \theta)$ and $\log \lambda_c(x_k \mid H_k, \theta)$ are twice differentiable functions that we denote generically as $g(x_k)$. To evaluate the first term on the right side of equation 3.4, it suffices to compute $E[g(x_k \mid H_k, \theta) \parallel H_K, \theta^{(\ell)}]$. This can be accomplished by expanding $g(x_k)$ in a Taylor series about $\hat{x}_{k|K}$ and taking the expected value to obtain the approximation

$$E[g(x_k \mid H_k, \theta) \parallel H_K, \theta^{(\ell)}] \doteq g(\hat{x}_{k|K}) + \frac{1}{2}\sigma^2_{k|K} g''(\hat{x}_{k|K}), \tag{3.5}$$

where $g''(\hat{x}_{k|K})$ is the second derivative of $g(x_k)$ evaluated at $\hat{x}_{k|K}$. The right-hand side of equation 3.5 is substituted into equation 3.4 to evaluate the E-step. The evaluation of the second term on the right of equation 3.4 proceeds as in the evaluation of the second and third terms on the right of equation 2.8.

If the log conditional intensity function is no longer a linear or approximately linear function of the parameters, the M-step takes the more

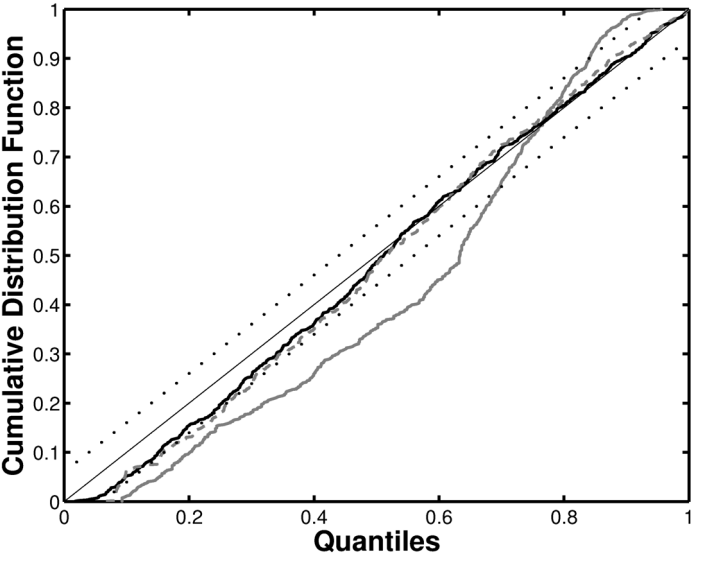

Figure 6: Kolmogorov-Smirnov goodness-of-fit analysis for local Bernoulli probability model. The K-S plot for the EM algorithm model-based estimate (dashed line) lies almost entirely within the 95% confidence bounds (dotted lines) and follows closely the KS plot computed using the true firing rate (solid black line), which lies almost entirely on the 45 degree line of exact agreement. In contrast, the empirical rate estimate (solid gray line) lies mostly outside the confidence limits, suggesting that this model does not agree closely with the data.

general form,

$$\nabla Q(\theta \mid \theta^{(\ell)}) = 0, \tag{3.6}$$

where the gradient in $\nabla Q(\theta \mid \theta^{(\ell)})$ is with respect to θ. The zero of $\nabla Q(\theta \mid \theta^{(\ell)})$ and, hence $\theta^{(\ell+1)}$, has to be found using Newton's method or another appropriate numerical optimization procedure. Similarly, the recursive filtering and smoothing algorithms generalize in a straightforward way when the dimension of the state-space model is greater than one (Brown et al., 1998). While these modifications increase the computational requirements of our algorithm, they illustrate how it can be applied to a wider range of point process and state-space models.

4 Discussion

We have presented a method for estimating from point process (spike train) data a conditional intensity (rate) function modulated by an unobservable

or latent continuous-valued state variable. The latent variable relates the effect of the external stimuli applied at specified times by the experimenter to the spike train rate function. We compute maximum likelihood estimates of the model parameters by the EM algorithm in which the E-step combines forward and backward point process filtering algorithms. The model performs better than smoothed histogram estimates of rate because it makes explicit use of the timing of the stimulus to analyze changes in background firing. Also, the model gives a more accurate description of the neural spike train as evaluated by the goodness-of-fit K-S test.

Several authors have discussed the analyses of state-space models in which the observation process is a point process. Diggle, Liang, and Zeger (1995) briefly mention state estimation from point process observations but no specific algorithms are given. MacDonald and Zucchini (1997) discuss state estimation for point processes without using the smoothing and filtering approach suggested here. West and Harrison (1997) define the state-space model implicitly and use the discount concept to construct an approximate forward filter. This approach is difficult to generalize (Fahrmeir, 1992). Kitagawa and Gersch (1996) described numerical algorithms to carry out state-space updating with forward recursion algorithms for binomial and Poisson observation processes. For the Poisson model in equation 2.6, Chan and Ledolter (1995) provided a computationally intensive Markov chain Monte Carlo EM algorithm to conduct the state updating and parameter estimation. The forward updating algorithms of Fahrmeir (1992), Fahrmeir and Tutz (1994), and Durbin and Koopman (2000) resemble most closely the ones we present, particularly, in the special case where the observation process is a point process from an exponential family, and the natural parameter is modeled as a linear function of the latent process. Both the examples we present follow these two special cases. The Fahrmeir forward recursion algorithm for example 1 with a single neuron is

$$x_{k|k} = x_{k|k-1} + \frac{\sigma^2_{k|k-1}\beta}{[\lambda(k\Delta)\beta^2\sigma^2_{k|k-1} + 1]}[dN(k\Delta) - \lambda(k\Delta)] \tag{4.1}$$

$$\sigma^2_{k|k} = [(\sigma^2_{k|k-1})^{-1} + \lambda(k\Delta)\beta^2]^{-1}, \tag{4.2}$$

whereas the Durbin and Koopman (2000) update is

$$x_{k|k} = x_{k|k-1} + \frac{\sigma^2_{k|k-1}\beta}{(\lambda(k\Delta) + \sigma^2_{k|k-1}\beta^2)\lambda(k\Delta)}[dN(k\Delta) - \lambda(k\Delta)] \tag{4.3}$$

$$\sigma^2_{k|k} = [(\sigma^2_{k|k-1})^{-1} + \beta^2\lambda(k\Delta)^{-1}]^{-1}. \tag{4.4}$$

The variance updating algorithm in the Fahrmeir algorithm agrees because the observed and expected Fisher information are the same for the Poisson model in our example. The state updating equation differs from our

updating formula in equation 2.15 because their update is computed from the Kalman filter and not directly by finding the root of the log posterior probability density. The state and variance update formulae in the Durbin and Koopman algorithm differ from ours because theirs use a Taylor series approximation of the score function, first derivative of the log likelihood, instead of the exact score function. Fahrmeir (1992) and Fahrmeir and Tutz (1994) suggest using the EM algorithm for estimating the unknown parameters, but details are not given.

In an example applied to spike train data, Sahini (1999) describes the use of a latent model for neural firing where spikes are generated as an inhomogeneous Polya process. In his model, parameters are computed by optimizing the marginalized posterior by gradient ascent, and Monte Carlo goodness-of-fit is used to compare the model fit with measured spike train stochastic process.

The fact that our state-space models fit the simulated data better than the empirical method is expected given that the spikes were generated with the model. In applications to real data, it will be possible to use the same approach, testing reasonable and ideally parsimonious forms of the state-space and point process models for a given neurophysiological experiment. In any case, we may use the time-rescaling theorem to assess goodness-of-fit of any candidate models.

To study the problem of estimating a latent process simultaneously with its model parameters and the parameters of the observation process, we discretized time and assumed that the observation process and the latent process occur on a lattice of points spaced Δ time units apart. Using the EM algorithm, we computed the maximum likelihood estimate of θ and empirical Bayes' estimates of the latent process conditional on the maximum likelihood estimate of θ. A Bayesian alternative would be to specify a prior distribution for θ and compute a joint posterior probability density for the latent process and θ. Liu and Chen (1998) developed sequential Monte Carlo algorithms that may be adapted to this approach.

As another alternative, it is useful to point out how the latent process and parameter estimation may be carried out if both the point process and the latent process are assumed to be measured in continuous time. Nonlinear continuous time filtering and smoothing algorithms for point process observations have been studied extensively in the control theory literature (Snyder, 1975; Segall, Davis, & Kailath, 1975; Boel & Beneš, 1980; Snyder & Miller, 1991; Twum-Danso, 1997; Solo, 2000; Twum-Danso & Brockett, 2001). If the normalized conditional probability density, $p(x(t) \mid N_{0,t})$, is to be evaluated in continuous time, then a nonlinear stochastic partial differential equation in this probability density must be solved at each step (Snyder, 1975; Snyder and Miller, 1991). Here we let $x(t)$ be the continuous time value of x_k. If the updating is performed with respect to the unnormalized conditional probability density, $p(x(t), N_{0,t})$, then a linear stochastic partial differential equation must be solved in this probability density at

each step (Boel & Beneš, 1980; Twum-Danso, 1997; Solo, 2000). For either the normalized or unnormalized probability density updating algorithms, the essential steps in their derivations use the posterior prediction equation in equation A.1 and the one-step prediction equation in equation A.2 to derive Fokker-Planck equations (Snyder, 1975; Snyder & Miller, 1991; Twum-Danso, 1997; Solo, 2000; Twum-Danso & Brockett, 2001). If the parameters of the continuous time system are nondynamic and unknown, then, as in the discretized time case we present here, either the normalized or unnormalized partial differential equation updating of the conditional probability density may be embedded in an EM algorithm to compute maximum likelihood estimates of the parameters and empirical Bayes estimates of the latent process. Similarly, a Bayesian procedure can be derived if a prior probability density for θ can be specified. While the normalized and unnormalized conditional probability density updating equations have been known for several years, the computational requirements of these algorithms may be the reason they have not been more widely used (Manton, Krishnamurthy, & Elliott, 1999). Discretized approximations (Snyder & Miller, 1991; Twum-Danso, 1997; Twum-Danso & Brockett, 2001) and sequential Monte Carlo algorithms (Solo, 2000; Doucet, de Freitas, & Gordon, 2001; Shoham, 2001) have been suggested as more plausible alternatives. The sequential Monte Carlo methods use simulations to compute recursively the solutions to equations A.1 and A.2 on a discrete lattice of time points, whereas our nonlinear recursive algorithm, equations 2.12 through 2.16, uses sequential gaussian approximations to perform the same computations.

A potential application of this analysis paradigm would be to estimate the effect of external cue on a spike train in the delayed-response hand-pointing task described in Riehle et al. (1997). In this experiment, parallel spike data, measured in primary motor cortex of the monkey, are analyzed to estimate differences between spike rate increases corresponding to actual motion and those caused by expectation of a stimulus. The structure of our model enables us to estimate above-random firing propensity in a single cell while incorporating the history of cell firing. For these reasons, this approach may have advantages over the unitary events analysis methods (Grün et al., 1999), which may be difficult to apply to neurons with low firing rates (Roy, Steinmetz, & Niebur, 2000). A second potential application would be in the analysis of cell firing in the trace conditioning paradigm (McEchron, Weible, & Disterhof, 2001). In this case, a conditioned stimulus is followed after a trace interval by an unconditioned stimulus. After many such trials, an association between the two stimuli develops, as evidenced by changes in the firing rate of the neuron. These data are conventionally analyzed using PSTH techniques. However, because these studies involve an implicit relation between the stimulus and the neural spiking activity, this relation may be more clearly delineated by using the paradigm presented here. Finally, we are currently investigating the application of these methods to learning and memory experiments during

recordings from the medial temporal lobe of the monkey (Wirth et al., 2002; Yanike et al., 2002).

The state-space approach suggests several advantages. First, the approach uses a latent variable to relate explicitly the timing of the stimulus input and history of the experiment to the observed spiking activity. Second, use of explicit probability models makes it possible to compute probability density functions and confidence intervals for model quantities of interest. Finally, formulation of the analysis in terms of a general point process model allows us to assess model goodness-of-fit using the K-S tests based on the time-rescaling theorem. In our opinion, this latter step is the most critical as it forces us to assess how sensitive our inferences may be to lack of agreement between the model and the experimental data.

In summary, we have presented a computationally tractable method for state-space and parameter estimation from point process observations and suggested that these algorithms may be useful for analyzing neurophysiologic experiments involving implicit stimuli. In a future publication, we will apply these methods to actual experimental studies.

Appendix: Derivation of the Recursive Nonlinear Filter Algorithm

We derive a form of the recursive filter equations appropriate for an arbitrary point process model. The algorithm in equations 2.12 through 2.16 is obtained by taking the special case of the Poisson. To derive the nonlinear recursive filter, we require the posterior prediction equation,

$$p(x_k \mid H_k) = \frac{p(x_k \mid H_{k-1})p(dN(k\Delta) \mid x_k, H_k)}{p(dN(k\Delta) \mid H_{k-1})}, \tag{A.1}$$

and the one-step prediction or Chapman-Kolmogorov equation,

$$p(x_k \mid H_{k-1}) = \int p(x_k \mid x_{k-1})p(x_{k-1} \mid H_{k-1})\, dx_{k-1}. \tag{A.2}$$

The derivation of the algorithm proceeds as follows. Assume that at time $(k-1)\Delta$, $x_{k-1|k-1}$ and $\sigma^2_{k-1|k-1}$ are given. Under a gaussian continuity assumption on x_k, the distribution of x_k given $x_{k-1|k-1}$ is $N(\rho x_{k-1|k-1} + \alpha I_k, \sigma^2_{k|k-1})$, where $\sigma^2_{k|k-1} = \sigma^2_\varepsilon + \rho^2\sigma^2_{k-1|k-1}$. By equations 2.4, A.1, and A.2 and the gaussian continuity assumption, the posterior probability density $p(x_k \mid H_k)$ and the log posterior probability density $\log p(x_k \mid H_k)$ are, respectively,

$$p(x_k \mid H_k) \propto \exp\left\{-\frac{1}{2}\frac{(x_k - \rho x_{k-1|k-1} - \alpha I_k)^2}{\sigma^2_{k|k-1}}\right\} \times \prod_{c=1}^{C} \exp\{\log\lambda_c(k\Delta \mid H^c_k)dN^c(k\Delta) - \lambda_c(k\Delta \mid H^c_k)\Delta\} \tag{A.3}$$

$$\log p(x_k \mid H_k) \propto -\frac{1}{2}\frac{(x_k - \rho x_{k-1|k-1} - \alpha I_k)^2}{\sigma^2_{k|k-1}} + \sum_{c=1}^{C}[\log \lambda_c(k\Delta \mid H_k^c)dN^c(k\Delta) - \lambda_c(k\Delta \mid H_k^c)\Delta]. \quad \text{(A.4)}$$

To find the optimal estimate of x_k, we apply a gaussian approximation to equation A.3. This gaussian approximation is distinct from the gaussian continuity assumption and means that we can use the mode and variance of the probability density in equation A.3 to approximate it as a gaussian probability density. As a result, we differentiate with respect to x_k to find the mode, and we compute the second derivative to obtain the approximate variance (Tanner, 1996). Differentiating equation A.4 with respect to x_k gives

$$\frac{\partial \log p(x_k \mid H_k)}{\partial x_k} = -\frac{(x_k - \rho x_{k-1|k-1} - \alpha I_k)}{\sigma^2_{k|k-1}} + \sum_{c=1}^{C}\frac{1}{\lambda_c(k\Delta)}\frac{\partial \lambda_c}{\partial x_k}[dN^c(k\Delta) - \lambda_c(k\Delta)\Delta], \quad \text{(A.5)}$$

and solving for x_k yields

$$x_k = \rho x_{k-1|k-1} + \alpha I_k + \sum_{c=1}^{C}\sigma^2_{k|k-1}\lambda_c(k\Delta \mid H_k^c)^{-1} \times \frac{\partial \lambda_c(k\Delta \mid H_k^c)}{\partial x_k}[dN^c(k\Delta) - \lambda_c(k\Delta \mid H_k^c)\Delta]. \quad \text{(A.6)}$$

Equation A.6 is in general nonlinear in x_k and can be solved using Newton's method. The second derivative of equation A.5 is

$$\frac{\partial^2 \log p(x_k \mid H_k)}{\partial x_k^2} = -\frac{1}{\sigma^2_{k|k-1}} + \sum_{c=1}^{C}\left[\left(\frac{\partial^2 \lambda_c(k\Delta)}{\partial x_k^2}\frac{1}{\lambda_c(k\Delta)} - \left(\frac{\partial \lambda_c(k\Delta)}{\partial x_k}\right)^2\frac{1}{\lambda_c(k\Delta)^2}\right) \times [dN^c(k\Delta) - \lambda_c(k\Delta)\Delta] - \left(\frac{\partial \lambda_c(k\Delta)}{\partial x_k}\right)^2\frac{1}{\lambda_c(k\Delta)}\Delta\right], \quad \text{(A.7)}$$

and the variance of x_k, under the gaussian approximation to equation A.3, is

$$\sigma^2_{k|k} = -\left[-\frac{1}{\sigma^2_{k|k-1}} + \sum_{c=1}^{C}\left[\left(\frac{\partial^2\lambda_c(k\Delta)}{\partial x_k^2}\frac{1}{\lambda_c(k\Delta)} - \left(\frac{\partial\lambda_c(k\Delta)}{\partial x_k}\right)^2\frac{1}{\lambda_c(k\Delta)^2}\right) \times [dN^c(k\Delta) - \lambda_c(k\Delta)\Delta] - \left(\frac{\partial\lambda_c(k\Delta)}{\partial x_k}\right)^2\frac{1}{\lambda_c(k\Delta)}\Delta\right]\right]^{-1}. \quad \text{(A.8)}$$

Equations A.6 and A.8 constitute the basis for the general form of the filter equations 2.12 through 2.16.

Acknowledgments

Support was provided in part by NIMH grants MH59733, MH61637, NIDA grant DA015644, NHLBI grant HL07901, and NSF grant IBN-0081458. Part of this research was performed while E.N.B. was on sabbatical at the Laboratory for Information and Decision Systems in the Department of Electrical Engineering and Computer Science at MIT.

References

Barbieri, R., Quirk, M. C., Frank, L. M., Wilson, M. A., & Brown, E. N. (2001). Construction and analysis of non-Poisson stimulus-response models of neural spike train activity. *J. Neurosci. Methods, 105,* 25–37.

Berry, M. J., Warland, D. K., & Meister, M. (1997). The structure and precision of retinal spike trains. *Proc. Nat. Acad. Sci. USA, 94,* 5411–5416.

Bialek, W., Rieke, F., de Ruyter van Steveninck, R. R., & Warland, D. (1991). Reading a neural code. *Science, 252,* 1854–1857.

Boel, R. K., & Beneš, V. E. (1980). Recursive nonlinear estimation of a diffusion acting as the rate of an observed Poisson process. *IEEE Trans. Inf. Theory, 26*(5), 561–574.

Brown, E. N. (1987). *Identification and estimation of differential equation models for circadian data.* Unpublished doctoral dissertation, Harvard University, Cambridge, MA.

Brown, E. N., Barbieri, R., Ventura, V., Kass, R. E., & Frank, L. M. (2002). The time-rescaling theorem and its application to neural spike train data analysis. *Neural Comp., 14*(2), 325–346.

Brown, E. N., Frank, L. M., Tang, D., Quirk, M. C., & Wilson, M. A. (1998). A statistical paradigm for neural spike train decoding applied to position prediction from ensemble firing patterns of rat hippocampal lace cells. *J. Neurosci., 18,* 7411–7425.

Chan, K. S., & Ledolter, J. (1995). Monte Carlo estimation for time series models involving counts. *J. Am. Stat. Assoc., 90,* 242–252.

Cox, D. R., & Isham, V. (1980). *Point processes*. New York: Chapman and Hall.
Daley, D. J., & Vere-Jones, D. (1988). *An introduction to the theory of point processes*. New York: Springer-Verlag.
de Jong, P., & Mackinnon, M. J. (1988). Covariances for smoothed estimates in state space models. *Biometrika, 75*, 601–602.
Dempster, A. P., Laird, N. M., & Rubin, D. B. (1977). Maximum likelihood from incomplete data via the EM algorithm (with discussion). *J. Roy. Statist. Soc. B, 39*, 1–38.
Diggle, P. J., Liang, K-Y., & Zeger, S. L. (1995). *Analysis of longitudinal data*. Oxford: Clarendon.
Doucet, A., de Freitas, N., & Gordon, N. (2001). *Sequential Monte Carlo methods in practice*. New York: Springer-Verlag.
Durbin, J., & Koopman, S. J. (2000). Time series analysis of non-gaussian observations based on state space models from both classical and Bayesian perspectives. *J. Roy. Statist. Soc. B, 62*, 3–56.
Fahrmeir, L. (1992). Posterior mode estimation by extended Kalman filtering for multivariate dynamic generalized linear models. *J. Am. Stat. Assoc., 87*, 501–509.
Fahrmeir, L., & Tutz, D. (1994). Dynamic-stochastic models for time-dependent ordered paired-comparison systems. *J. Am. Stat. Assoc., 89*, 1438–1449.
Gharamani, Z. (2001). An introduction to hidden Markov models and Bayesian networks. *Int. J. Pattern Recognition, 15*(1), 9–42.
Grün, S., Diesmann, M., Grammont, F., Riehle A., & Aertsen, A. (1999). Detecting unitary events without discretization of time. *J. Neurosci. Meth., 93*, 67–79.
Kalbfleisch, J. D., & Prentice, R. L. (1980). *The statistical analysis of failure time data*. New York: Wiley.
Kay, S. M. (1988). *Modern spectral estimation: Theory and applications*. Upper Saddle River, NJ: Prentice Hall.
Kitagawa, G., & Gersh, W. (1996). *Smoothness priors analysis of time series*. New York: Springer-Verlag.
Liu, J. S., & Chen, R. (1998). Sequential Monte Carlo methods for dynamic systems. *J. Am. Stat. Assoc., 93*(443), 567–576.
Ljung, L., & Söderström, S. (1987). *Theory and practice of recursive identification*. Cambridge, MA: MIT Press.
MacDonald, I. L., & Zucchini, W. (1997). *Hidden Markov and other models for discrete-valued time series*. New York: Chapman and Hall.
Manton, J. H., Krishnamurthy, V., & Elliott, R. J. (1999). Discrete time filters for doubly stochastic Poisson processes and other exponential noise models. *Int. J. Adapt. Control Sig. Proc., 13*, 393–416.
McEchron, M. D., Weible, A. P., & Disterhoft, J. F. (2001). Aging and learning-specific changes in single-neuron activity in CA1 hippocampus during rabbit trace eyeblink conditioning. *J. Neurophysiol., 86*, 1839–1857.
Mendel, J. M. (1995). *Lessons in estimation theory for signal processing, communication, and control*. Upper Saddle River, NJ: Prentice Hall.
O'Keefe, J., & Dostrovsky, J. (1971). The hippocampus as a spatial map: preliminary evidence from unit activity in the freely-moving rat. *Brain Research, 34*, 171–175.

Riehle, A., Grün, S., Diesmann, M., & Aertsen, A. (1997). Spike synchronization and rate modulation differentially involved in motor cortical function. *Science, 278*, 1950–1953.

Roweis, S., & Ghahramani, Z. (1999). A unifying review of linear gaussian models. *Neural Comp., 11*, 305–345.

Roy, A., Steinmetz, P. N., & Niebur, E. (2000). Rate limitations of unitary event analysis. *Neural Comp., 12*(9), 2063–2082.

Sahini, M. (1999). *Latent variable models for neural data analysis*. Unpublished doctoral dissertation, California Institute of Technology, Pasadena.

Segall, A., Davis, M. H. A., & Kailath, T. (1975). Nonlinear filtering with counting observations. *IEEE Trans. Inf. Theory, 21*(2), 143–149.

Shoham, S. (2001). *Advances towards an implantable motor cortical interface*. Unpublished doctoral dissertation, University of Utah, Salt Lake City.

Shumway, R. H., & Stoffer, D. S. (1982). An approach to time series smoothing and forecasting using the EM algorithm. *J. Time Series Analysis, 3*, 253–264.

Snyder, D. (1975). *Random point processes*. New York: Wiley.

Snyder, D. L., & Miller, M. I. (1991). *Random point processes in time and space*. New York: Springer-Verlag.

Solo, V. (2000). Unobserved Monte-Carlo method for identification of partially-observed nonlinear state-space systems, part II: counting process observations. In *Proc. IEEE Conference on Decision and Control*. New York: Institute of Electrical and Electronic Engineers.

Tanner, M. A. (1996). *Tools for statistical inference*. New York: Springer-Verlag.

Twum-Danso, N. T. (1997). *Estimation, information and neural signals*. Unpublished doctoral dissertation, Harvard University, Cambridge, MA.

Twum-Danso, N. T., & Brockett, R. (2001). Trajectory information from place cell data. *Neural Networks, 14*(6–7), 835–844.

West, M., & Harrison, J. (1997). *Bayesian forecasting and dynamic models*. New York: Springer-Verlag.

Wilson, M. A., & McNaughton, B. L. (1993). Dynamics of the hippocampal ensemble code for space. *Science, 261*, 1055–1058.

Wirth, S., Chiu, C., Sharma, V., Frank, L. M., Smith, A. C., Brown, E. N., & Suzuki, W. A. (2002). *Medial temporal lobe activity during the acquisition of new object-place associations*. Program 676.1, 2002 Abstract Viewer/Itinerary Planner, Society for Neuroscience. Available on-line: http://sfn.scholarone.com.

Wood, E. R., Dudchenko, P. A., & Eichenbaum, H. (1999). The global record of memory in hippocampal neuronal activity. *Nature, 397*(6720), 613–616.

Yanike, M., Wirth, S., Frank, L. M., Smith, A. C., Brown, E. N., & Suzuki, W. A. (2002). *Categories of learning-related cells in the primate medial temporal lobe*. Program 676.2, 2002 Abstract Viewer/Itinerary Planner, Society for Neuroscience. Available on-line: http://sfn.scholarone.com.

Received April 24, 2002; accepted November 18, 2002.